

## Design and Fabrication of a High-Performance Electrochemical Glucose Sensor

Santhisagar Vaddiraju, Ph.D.,<sup>1,2</sup> Allen Legassey, B.S.,<sup>2</sup> Yan Wang, M.S.,<sup>3</sup>  
Liangliang Qiang, M.S.,<sup>1</sup> Diane J. Burgess, Ph.D.,<sup>3</sup> Faquir Jain, Ph.D.,<sup>4</sup>  
and Fotios Papadimitrakopoulos, Ph.D.<sup>1,5</sup>

### Abstract

#### Objective:

Development of electrochemical sensors for continuous glucose monitoring is currently hindered by a variety of problems associated with low selectivity, low sensitivity, narrow linearities, delayed response times, hysteresis, biofouling, and tissue inflammation. We present an optimized sensor architecture based on layer stratification, which provides solutions that help address the aforementioned issues.

#### Method:

The working electrode of the electrochemical glucose sensors is sequentially coated with five layers containing: (1) electropolymerized polyphenol (PPh), (2) glutaraldehyde-immobilized glucose oxidase ( $\text{GO}_x$ ) enzyme, (3) dip-coated polyurethane (PU), (4) glutaraldehyde-immobilized catalase enzyme, and (5) a physically cross linked polyvinyl alcohol (PVA) hydrogel membrane. The response of these sensors to glucose and electroactive interference agents (i.e., acetaminophen) was investigated following application of the various layers. Sensor hysteresis (i.e., the difference in current for a particular glucose concentration during ascending and descending cycles after 200 s) was also investigated.

#### Results:

The inner PPh membrane improved sensor selectivity via elimination of electrochemical interferences, while the third PU layer afforded high linearity by decreasing the glucose-to- $\text{O}_2$  ratio. The fourth catalase layer improved sensor response time and eliminated hysteresis through active withdrawal of  $\text{GO}_x$ -generated  $\text{H}_2\text{O}_2$  from the inner sensory compartments. The outer PVA hydrogel provided mechanical support and a continuous pathway for diffusion of various participating species while acting as a host matrix for drug-eluting microspheres.

#### Conclusions:

Optimal sensor performance has been achieved through a five-layer stratification, where each coating layer works complementarily with the others. The versatility of the sensor design together with the ease of fabrication renders it a powerful tool for continuous glucose monitoring.

*J Diabetes Sci Technol* 2011;5(5):1044-1051

**Author Affiliations:** <sup>1</sup>Polymer Program, Institute of Materials Science, University of Connecticut, Storrs, Connecticut; <sup>2</sup>Biorasis, Inc., Technology Incubation Program, University of Connecticut, Storrs, Connecticut; <sup>3</sup>School of Pharmacy, University of Connecticut, Storrs, Connecticut; <sup>4</sup>Electrical and Computer Engineering, University of Connecticut, Storrs, Connecticut; and <sup>5</sup>Department of Chemistry, University of Connecticut, Storrs, Connecticut

**Abbreviations:** (AP) acetaminophen, (BSA) bovine serum albumin, (FAD) flavin adenine dinucleotide, ( $\text{GO}_x$ ) glucose oxidase, (PBS) phosphate-buffered saline, (PPh) polyphenol, (PU) polyurethane, (PVA) polyvinyl alcohol

**Keywords:** bienzymatic, biosensor lag time, drug delivery coatings, foreign body response, implantable glucose sensors, outer membranes, selectivity

**Corresponding Author:** Fotios Papadimitrakopoulos, Ph.D., Polymer Program, Institute of Material Science, U-3136, University of Connecticut, Storrs, CT 06269; email address [papadim@mail.ims.uconn.edu](mailto:papadim@mail.ims.uconn.edu)

**D**evelopment of reliable glucose sensors for continuous glucose monitoring is a critical step toward development of an artificial pancreas.<sup>1–3</sup> In view of this, glucose detection based on electrochemical, near-infrared, Raman, fluorescence, and piezoelectric technology as well as various other transduction mechanisms are actively being investigated, with the common goal of achieving stable and reliable performance.<sup>2,4</sup> High specificity of the glucose oxidase (GO<sub>x</sub>) enzyme toward *D*-glucose along with their ease of miniaturization has propelled Clark-type electrochemical sensors to the forefront of continuous glucose monitoring devices.<sup>5–7</sup> These sensors typically involve amperometric detection of various electroactive species [i.e., H<sub>2</sub>O<sub>2</sub>, O<sub>2</sub> and redox mediators coupled with the flavin adenine dinucleotide (FAD) co-factor of GO<sub>x</sub>] according to reactions (1) and (2):<sup>8</sup>



Despite the straightforwardness of reactions (1) and (2), a number of problems arise when the complexity of body physiology is intertwined with the actual sensor element. Some of these problems include

- (a) the presence of various endogenous (ascorbic acid, uric acid) and exogenous [acetaminophen (AP)] species that are redox active at the sensor operating potential;<sup>5,9</sup>
- (b) signal saturation due to lower oxygen-to-glucose concentrations (by one to two orders of magnitude in normal to hyperglycemic conditions, respectively), as per reactions (1) and (2);<sup>5,9</sup>
- (c) implantation-driven body responses to the sensor, which lead to biofouling, inflammation, and eventual fibrosis<sup>10–12</sup> (these typically impede mass transfer of glucose and O<sub>2</sub> to the inner sensor compartments housing the GO<sub>x</sub> and eventually result in degradation of sensor sensitivity);<sup>11</sup> and
- (d) mass transfer-based limitations inherent to the sensor design that lead to delayed sensor response time and large hysteresis.<sup>2,9,13</sup>

These problems have led researchers to investigate different strategies (such as the use of various membranes,<sup>7,8</sup> drug-delivering coatings,<sup>12,14–18</sup> nanomaterials,<sup>9,19,20</sup> and

mediators<sup>21–26</sup>) in order to improve sensor performance. These strategies, while solving one or more problems, typically exacerbate mass transfer problems of the various participating species (e.g., glucose, O<sub>2</sub>, H<sub>2</sub>O<sub>2</sub>). Moreover, in the case of mediators and nanomaterials, issues of possible toxicity may arise should they leach out.<sup>9,27,28</sup> Accordingly, our group is evaluating mediator-free, first-generation Clark-type sensors that rely solely on careful mass transfer balance of various species involved in operating these devices.

In this article, we present an optimized sensor architecture that addresses most of the aforementioned issues. Optimal performance can be achieved through careful layer stratification of five layers, four of which alleviate limitations at the site where they occur, i.e., (1) an electro- to improve sensor selectivity via elimination of electrochemical interferences, (2) a semipermeable membrane on top of the GO<sub>x</sub>-containing layer to limit glucose flux and afford high sensor linearity, (3) a subsequent catalase-loaded layer to actively withdraw H<sub>2</sub>O<sub>2</sub> from the inner GO<sub>x</sub> layer and improve sensor response time while eliminating hysteresis, and (4) a thick outer hydrogel layer to provide mechanical support and act as a host for eventual incorporation of drug-delivery microspheres that have been shown to reduce inflammation and fibrosis.<sup>14,15,18,29</sup>

## Experimental Details

### Materials

Glucose oxidase enzyme (E.C. 1.1.3.4, 157 U/mg, *Aspergillus Niger*), catalase (E.C. 1.11.1.6, 5000 U/mg), glutaraldehyde (25% weight/volume solution in water), phenol, bovine serum albumin (BSA), glutaraldehyde (50% weight/volume), and *D*-glucose (reagent grade) were purchased from Sigma. Polyvinyl alcohol (PVA; 99% hydrolyzed, molecular weight 133 kDa) was obtained from Polysciences, Inc. (Warrington, PA). Platinum and silver wires were purchased from World Precision Instruments.

### Experimental Methods

#### Preparation of Polyvinyl Alcohol Solutions

Five percent weight/volume aqueous solution of 99% hydrolyzed PVA was preheated to approximately 80 °C to facilitate complete polymer dissolution.

#### Coil-Type Glucose Sensors

The working electrode was made by coiling a 125 μm Pt wire. The reference electrode was made by coiling

a 125  $\mu\text{m}$  silver wire in close proximity to the working electrode. The surface of the silver wire was subsequently converted to AgCl via galvanometry (at 0.4 V versus standard calomel electrode for 5 min) in a stirred 0.1 M HCl solution to render the Ag/AgCl reference electrode.

The total surface area of the Pt working electrode is approximately 2 mm<sup>2</sup>. This was first electrochemically cleaned in a 0.5 M H<sub>2</sub>SO<sub>4</sub> solution via potential cycling between -0.21 and 1.25 V until a stable background was reached.<sup>30</sup> Next, a film of polyphenol (PPh) was electropolymerized on the working electrode from an aqueous phenol solution.<sup>31</sup> Subsequently, the GO<sub>x</sub> enzyme was immobilized by dip coating the Pt/PPh electrode from a solution of 140 mg/ml GO<sub>x</sub>, 56 mg/ml BSA, and 25% weight/volume glutaraldehyde, the latter of which enables enzyme cross linking, followed by a 2 h soak in phosphate-buffered saline (PBS) to remove the uncross-linked proteins.<sup>32</sup>

The next step involved dip coating the sensor with a polyurethane (PU) layer from a 3% (weight/weight) PU solution in 98% tetrahydrofuran/2% dimethylformamide (weight/weight).<sup>33</sup> Subsequently, a thin layer of catalase enzyme was added by coating it with a solution of catalase, BSA, and glutaraldehyde, followed by another 2 h soak in PBS to remove the uncross-linked proteins. Finally, the sensor was encased within a thick (250  $\mu\text{m}$ ) PVA hydrogel and subjected to three freeze–thaw cycles to induce physical cross linking of PVA.<sup>34</sup>

### In Vitro Amperometric Experiments

*In vitro* amperometric experiments were performed in a stirred PBS solution (pH 7.4) maintained at 37 °C and under an applied potential of 0.7 V versus an Ag/AgCl reference electrode using a CH Instruments (Model CHI1010A) electrochemical analyzer.

Sensor response current versus various glucose concentrations were performed by raising the glucose levels in the test cell by 2 mM every 100 s for up to 30 mM, following an initial background stabilization period of ~8 min. Similarly, the sensor response current to 0.1 mM of AP was noted to assess its selectivity as a model interference agent.

### Temperature Dependence of Sensor Sensitivity

Temperature dependence of sensor sensitivity was obtained by measuring the sensor responses to sequential glucose increments from 5.6 to 13.1 mM in a stirred PBS solution maintained at the desired temperature.

### Sensor Response Time and Hysteresis

Sensor response time and hysteresis were obtained by assessing the sensor response at 200 s (in the case of hysteresis) following sequential glucose increments and decrements (from 2 to 25 mM and back to 2 mM). To estimate response time, the time taken for the sensor to reach 90% of its saturation response current was noted for the aforementioned glucose cycles.

### Statistical Analysis

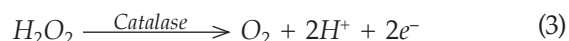
At least three sensors of each kind were fabricated, and results are presented as mean  $\pm$  standard deviation.

## Results and Discussion

### Glucose Sensor Design

**Figure 1** schematically illustrates the cross section of the electrochemical glucose sensor under study. The Pt working electrode was coated with a thin (approximately 10 nm) electropolymerized PPh layer to prevent oxidation of the large molecular weight electrochemical active species (i.e., AP, ascorbic acid, uric acid). These species are likely to oxidize at the operating potential (0.7 V versus Ag/AgCl) of the sensor.<sup>7</sup> The electrode was then decorated with GO<sub>x</sub> enzyme that was immobilized via cross linking with glutaraldehyde. Subsequently, the device was dip coated with PU to yield a conformal 3  $\mu\text{m}$  film on top of the GO<sub>x</sub> layer. This PU film was used to offset the large glucose-to-O<sub>2</sub> ratio within the subcutaneous tissue (typically 30 to 300 in normal versus hyperglycemic conditions) and render the sensor linear within the physiological glucose concentration (2 to 22 mM).<sup>33</sup>

Our prior research has indicated that precise control over the rate of outward diffusion of GO<sub>x</sub>-generated H<sub>2</sub>O<sub>2</sub> is important for maintaining adequate sensor sensitivity, fast response times, and minimal hysteresis.<sup>13,35</sup> This is because inward diffusion of glucose and O<sub>2</sub> are driven by the presence of the GO<sub>x</sub> enzyme, while outward diffusion of H<sub>2</sub>O<sub>2</sub> is solely influenced by the permeability of the PU membrane. Consequently, as the PU membrane provides a diffusion barrier to large molecules such as glucose, it also slows down the outward diffusion rate of H<sub>2</sub>O<sub>2</sub>. In this article, we introduce an additional driving force for outward diffusion of H<sub>2</sub>O<sub>2</sub> by applying a thin layer of catalase on top of the PU membrane, which converts H<sub>2</sub>O<sub>2</sub> to O<sub>2</sub> according to reaction (3):



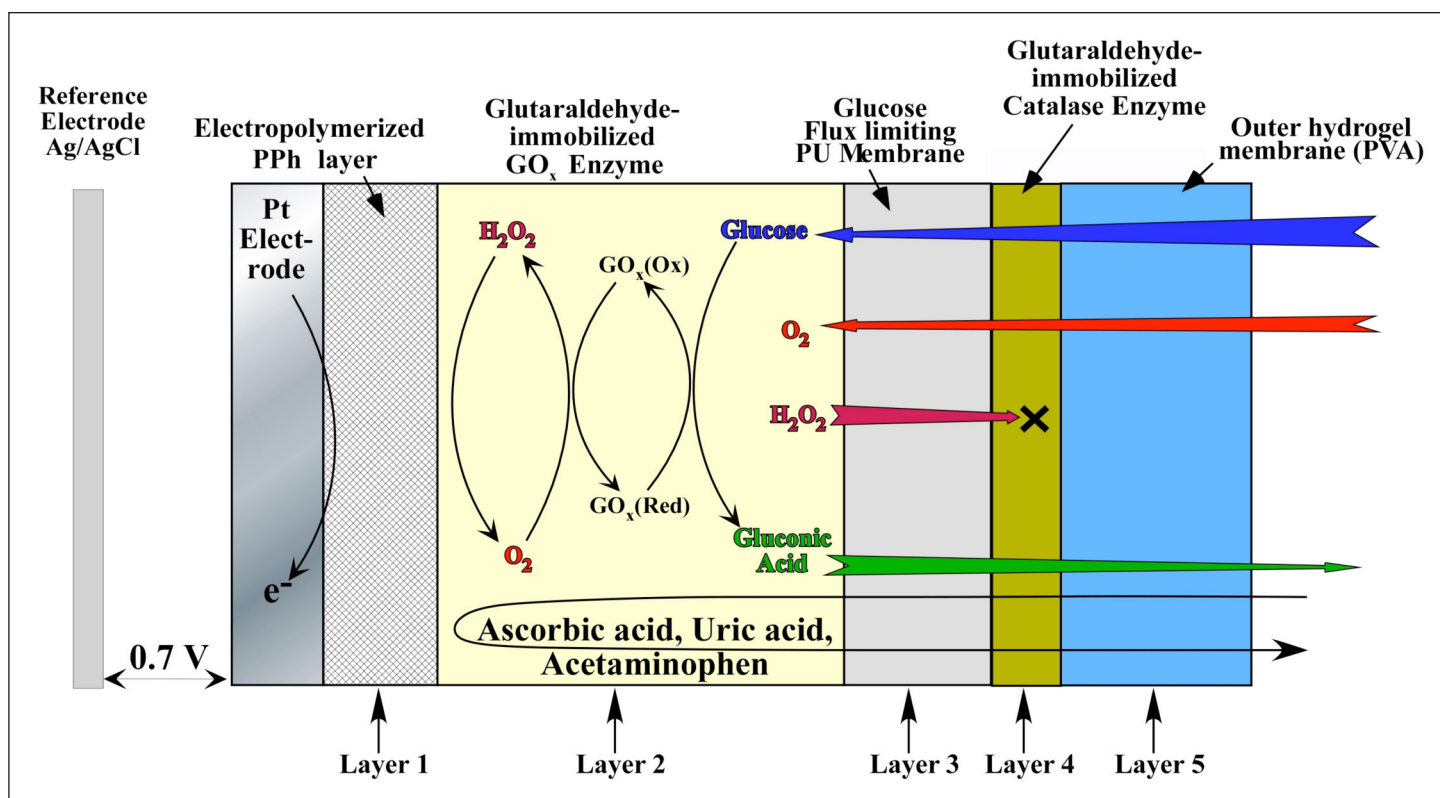


Figure 1. Schematic cross section of the sensor under investigation (layer thicknesses are not to scale).

Because the turnover rate of catalase is 40 times greater than  $\text{GO}_x$ ,<sup>36</sup> this can provide an effective means for removing  $\text{H}_2\text{O}_2$  from the interior of the sensor. In addition, this can also prevent possible tissue irritation by  $\text{H}_2\text{O}_2$  leaking out from the sensor to surrounding tissue.<sup>37</sup>

Following the catalase layer, the device was encased within a thick ( $250\ \mu\text{m}$ ) PVA hydrogel matrix that was cross linked in place through application of three repetitive freezing and thawing cycles.<sup>34</sup> This is achieved through freeze-induced water microcrystallization that causes partial PVA dehydration and subsequent formation of ordered domains that act as physical cross links.<sup>34</sup> This PVA hydrogel, aside from providing an outer mechanical stability to the inner layers, also acts as a host for a variety of tissue response modifiers that are typically released from the degradation of poly(lactic-co-glycolic acid) microspheres.<sup>14,15,18,34</sup> It has previously been established that such PVA hydrogels form a continuous pathway for glucose diffusion toward the inner layers of the working electrode as well as for outward diffusion of various enzymatic byproducts and tissue response modifiers.<sup>34,38</sup>

### Sensor Selectivity

Unlike ascorbic acid and uric acid, which are charged moieties and can be easily be blocked by similar polarity

layers (i.e., anionic NAFION<sup>30</sup>), AP being a noncharged molecule presents the biggest challenge.<sup>7</sup> Therefore, we chose acetaminophen as a model compound to investigate sensor selectivity. Figure 2 illustrates the amperometric response of the glucose sensor shown in Figure 1 (without the third, fourth, and fifth layers) on

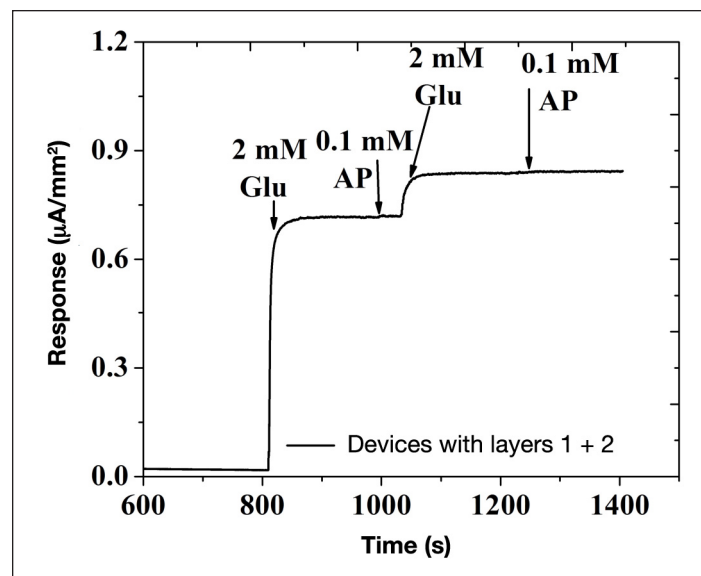


Figure 2. Amperometric response of Pt/PPh/ $\text{GO}_x$  sensors (without the third, fourth, and fifth layers) to sequential additions of 2 mM glucose and 0.1 mM AP, when operated at 0.7 V versus Ag/AgCl reference electrode. Glu, glucose; AP, acetaminophen.

sequential additions of 2 mM of glucose and 0.1 mM of acetaminophen (operated at 0.7 V versus Ag/AgCl reference electrode). As observed in **Figure 2**, the sensor shows a distinct increase upon addition of glucose and negligible to no response upon addition of acetaminophen (i.e., less than 2% of its amperometric response on bare Pt electrode; data not shown). This indicates that the pores of electropolymerized PPh layer are sufficiently large to allow small-sized  $\text{H}_2\text{O}_2$  to pass through but small enough to prevent diffusion of larger-sized acetaminophen. This renders the sensor highly selective. Here it should be noted that the nonlinear glucose response exhibited by the sensor in **Figure 2** is caused by the absence of outer flux limiting membranes (discussed later).

### Sensor Linearity and Sensitivity:

**Figure 3** shows amperometric response versus glucose for the sensor geometry of **Figure 1** terminated at various coating layers. Glucose sensors with layers 1 and 2 show the highest glucose sensitivity, yet poor linearity (these sensors begin to saturate at approximately 2 mM of glucose). This is also apparent from the glucose response of **Figure 2**, where evidence of signal saturation begins as low as 2 mM of glucose. This is due to insufficient amount of dissolved oxygen in the PBS medium as compared with the glucose concentration, which, in turn, limits cosubstrate supply to the  $\text{GO}_x$  according to reactions (1) and (2).<sup>39</sup> Upon application of 3  $\mu\text{m}$  of PU (layer 3), the device gains superb linearity for glucose concentrations as high as 30 mM. This comes at the expense of 65% lowered sensitivity (evident by the different abscissa used in **Figure 3**). Addition of catalase (layer 4) and PVA (layer 5) show no changes in linearity, which is still maintained beyond 30 mM of glucose. However, addition of catalase and PVA layers resulted in a 30% and 40% decrease in amperometric current versus that of the PU-terminated device. This indicates that, unlike PU, both catalase and PVA layers impose a minimal mass transfer barrier to both glucose and  $\text{O}_2$ . This is particularly true for PVA hydrogel, whose thickness is 80 times larger than that of the PU layer.

### Sensor Response Time and Hysteresis

Sensor response time is defined as the time taken to reach 90% of the saturation amperometric response for a particular glucose concentration. This parameter is related to mass transfer barriers that the layers impose on diffusion of substrate (glucose), cosubstrate (oxygen), and various enzymatic byproducts (e.g.,  $\text{H}_2\text{O}_2$ , glucuronolactone, gluconic acid) to attain equilibrium upon a change in glucose levels. In the case of

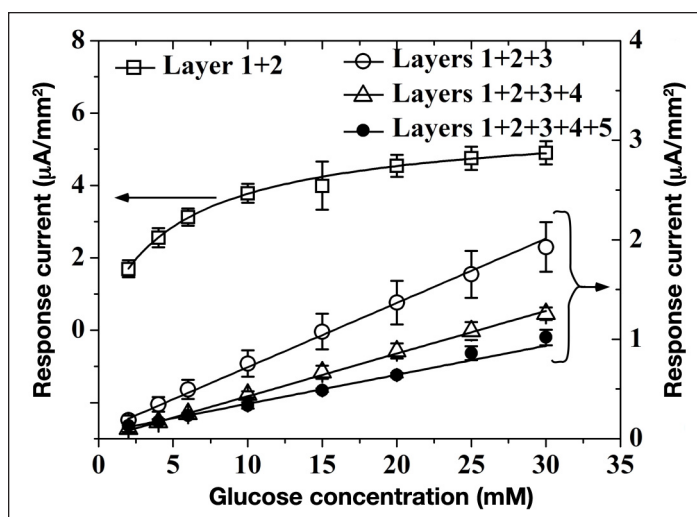


**Figure 3.** Saturation amperometric current versus glucose concentration for the device of **Figure 1** terminated at the various coating layers.

subcutaneous implantable glucose sensors, additional lag between interstitial and blood glucose events imposed by subcutaneous mass transfer considerations further exacerbate the apparent sensor response time. Typically, *in vitro* response time of Clark-type sensors is 2–5 min<sup>40</sup> while the lag between blood and interstitial fluid increases equilibration time to 5–12 min.<sup>41</sup> Moreover, sensor response further worsens as a result of biofouling and fibrosis.<sup>11</sup> Based on this, lowering mass transfer barriers within the sensor is directly reflected on improving the response time.

**Figure 4(A)** shows the response of the five-layer sensor (**Figure 1**) when subjected to sequential increments and decrements in glucose. Following each glucose addition step, sensor response time is approximately 60 s. Based on previous reports, this value appears to be 15% lower than similar sensors without the fourth catalase layer.<sup>40</sup> To further quantify the role of catalase, the hysteresis of this sensor geometry was investigated with and without the catalase layer. **Figure 4(b)** shows the 200 s response current for ascending and descending glucose cycles. Here, hysteresis is defined as the difference between the amperometric currents from the forward and backward cycles 200 s following the glucose injection.<sup>13</sup> In the case of sensors with no catalase [**Figure 4(B)(i)**], a 15–20% hysteresis is observed. On the other hand, upon insertion of the fourth catalase layer, the hysteresis falls below 5–8% [**Figure 4(B)(ii)**].

The profound effect of the catalase layer on sensor hysteresis provides a qualitative insight into the mass transfer of various participating species within the

sensor geometry. Based on careful control of layer 3 permeability (tuned via sequential layer-by-layer assembly), our prior investigations have indicated that sensor hysteresis is closely related to the outward diffusion rate of  $\text{H}_2\text{O}_2$ .<sup>13,35</sup> This, together with the high turnover rate of catalase for  $\text{H}_2\text{O}_2$  conversion to  $\text{O}_2$ , suggests that the observed hysteresis improvement are directly related to (1) efficient withdrawal of  $\text{H}_2\text{O}_2$  from the inner sensor compartments and (2) facile equilibration of glucose and  $\text{O}_2$  across both sides of the PU membrane. This can easily be comprehended as facilitating the work of  $\text{GO}_x$  by providing a catalase-induced means to remove one of its byproducts ( $\text{H}_2\text{O}_2$ ), while hydrolysis of glucuronolactone to gluconic acid removes the other byproduct. Consequently, the  $\text{GO}_x$ -driven inward diffusion of glucose and  $\text{O}_2$  is balanced by the catalase-facilitated outward diffusion of  $\text{H}_2\text{O}_2$ . This directly translates to both speeding up the sensor response and decreasing hysteresis, as shown in **Figure 4**.

### Temperature Dependence

An ideal glucose sensor should not be responsive to temperature changes as a result of physiological conditions such as hypothermia and hyperthermia.<sup>42</sup> The response of sensors (shown in **Figure 1**) could be affected by temperature increases due to (1) enhanced enzymatic activity, (2) increased membrane permeability of various participating species, and (3) decrease in dissolved  $\text{O}_2$  concentration.<sup>43</sup> **Figure 5** shows sensor sensitivity in the presence and absence of the outer three layers, which constitute semipermeable barriers that control the mass balance of key participating species (glucose,  $\text{O}_2$ , and  $\text{H}_2\text{O}_2$ ). Sensors with no semipermeable outer membranes show a super-linear increase in sensitivity at the rate of 5% to 7% per degree change in ambient temperature. On the other hand, sensors that employ the outer PU/catalase/PVA layers showed negligible temperature dependence in sensitivity. This is due to their reduced sensitivity (67% to 74%), which mostly results from a substantial reduction in inward diffusion of glucose. This renders the  $\text{GO}_x$  substrate well below its Michaelis-Menten constant, thereby allowing it to operate within its linear range where minimal temperature dependence is anticipated.

### Conclusions

A stratified layer design has been presented in order to address a variety of problems associated with first-generation Clark-based electrochemical glucose sensors. This involves sequential deposition of five layers, namely, (1) PPh, (2)  $\text{GO}_x$  enzyme, (3) PU, (4) catalase enzyme, and

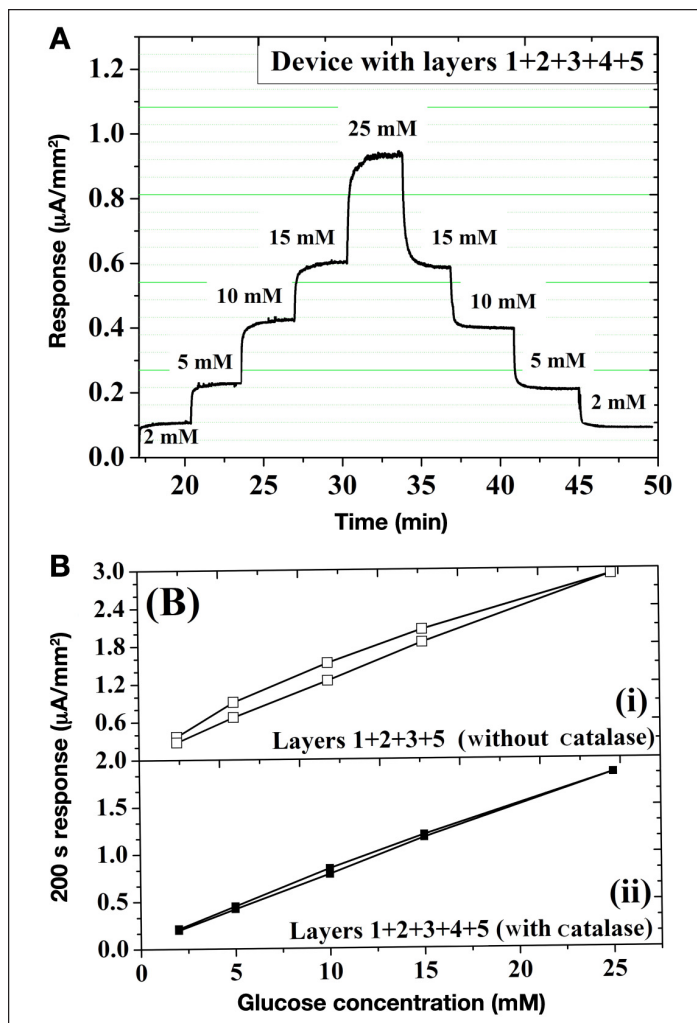


**Figure 4.** (A) Amperometric current of the five-layer sensor of **Figure 1** for sequential increase and decrease in glucose concentration. (B) Hysteresis analysis of saturation amperometric current versus glucose concentration for sensors (i) without and (ii) with the fourth catalase layer.

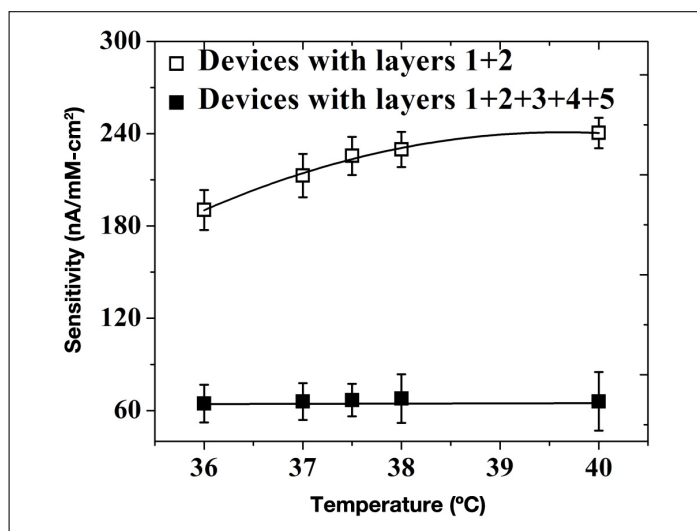


**Figure 5.** Sensitivity as a function of temperature for devices terminated at the various coating layers.

(5) PVA hydrogel. The PPh layer afforded high sensor selectivity by eliminating electrochemical interferences via permselective exclusion of species larger than  $\text{H}_2\text{O}_2$ . The PU layer formed an ideal flux-limiting membrane for glucose that balances  $\text{O}_2$  to glucose levels encountered in the entire glycemic range (2 to 22 mM) and beyond (up to 30 mM of glucose). Incorporation of the catalase layer on top of PU provided an additional driving force for withdrawing  $\text{H}_2\text{O}_2$  from the inner sensory compartments, thereby reducing sensor response time and minimizing hysteresis. Last but not least, the thick outer PVA hydrogel layer provides mechanical stability to the entire sensor and has been shown to be a versatile host for incorporating a variety of tissue-response modifiers, suitable for sustained delivery.<sup>14,15,18</sup> This stratified architecture provides a simplistic yet holistic approach to addressing various issues encountered with first-generation Clark-based glucose sensors, which avoids the need for resorting to redox mediators.

#### Funding:

Financial support for this study was obtained from U.S. Army medical research Grants W81XWH-09-1-0711 and W81XWH-07-10668, National Institutes of Health Grant 1-R21-HL090458-01, and Small Business Innovation Research Grants from National Science Foundation #1046902 and National Institutes of Health Grant R43EB011886.

#### References:

- Robert JJ. Continuous monitoring of blood glucose. *Horm Res.* 2002;57 Suppl 1:81–4.
- Vaddiraju S, Burgess DJ, Tomazos I, Jain FC, Papadimitrakopoulos F. Technologies for continuous glucose monitoring: current problems and future promises. *J Diabetes Sci Technol.* 2010;4(6):1540–62.
- Wang J. *In vivo* glucose monitoring: towards 'Sense and Act' feedback-loop individualized medical systems. *Talanta.* 2008;75(3):636–41.
- Oliver NS, Toumazou C, Cass AE, Johnston DG. Glucose sensors: a review of current and emerging technology. *Diabet Med.* 2009;26(3):197–210.
- Wang J. Glucose biosensors: 40 years of advances and challenges. *Electroanalysis.* 2001;13(12): 983–8.
- Wang J. Electrochemical biosensors: towards point-of-care cancer diagnostics. *Biosens Bioelectron.* 2006;21(10):1887–92.
- Wilson GS, Gifford R. Biosensors for real-time *in vivo* measurements. *Biosens Bioelectron.* 2005;20(12):2388–403.
- Wang J. Electrochemical glucose biosensors. *Chem Rev.* 2008;108(2):814–25.
- Vaddiraju S, Tomazos I, Burgess DJ, Jain FC, Papadimitrakopoulos F. Emerging synergy between nanotechnology and implantable biosensors: a review. *Biosens Bioelectron.* 2010;25(7):1553–65.
- Onuki Y, Bhardwaj U, Papadimitrakopoulos F, Burgess DJ. A review of the biocompatibility of implantable devices: current challenges to overcome foreign body response. *J Diabetes Sci Technol.* 2008;2(6):1003–15.
- Wisniewski N, Klitzman B, Miller B, Reichert WM. Decreased analyte transport through implanted membranes: differentiation of biofouling from tissue effects. *J Biomed Mater Res.* 2001;57(4):513–21.
- Wisniewski N, Reichert M. Methods for reducing biosensor membrane biofouling. *Colloids Surf B Biointerfaces.* 2000;18(3-4):197–219.
- Tipnis R, Vaddiraju S, Jain F, Burgess DJ, Papadimitrakopoulos F. Layer-by-layer assembled semipermeable membrane for amperometric glucose sensors. *J Diabetes Sci Technol.* 2007;1(2):193–200.
- Bhardwaj U, Sura R, Papadimitrakopoulos F, Burgess DJ. PLGA/PVA hydrogel composites for long-term inflammation control following s.c. implantation. *Int J Pharm.* 2010;384(1-2):78–86.
- Bhardwaj U, Sura R, Papadimitrakopoulos F, Burgess DJ. Controlling acute inflammation with fast releasing dexamethasone-PLGA microsphere/pva hydrogel composites for implantable devices. *J Diabetes Sci Technol.* 2007;1(1):8–17.
- Norton LW, Koschwanetz HE, Wisniewski NA, Klitzman B, Reichert WM. Vascular endothelial growth factor and dexamethasone release from nonfouling sensor coatings affect the foreign body response. *J Biomed Mater Res A.* 2007;81(4):858–69.
- Norton LW, Yuan F, Reichert WM. Glucose recovery with bare and hydrogel-coated microdialysis probes: experiment and simulation of temporal effects. *Anal Chem.* 2007;79(2):445–52.
- Patil SD, Papadimitrakopoulos F, Burgess DJ. Concurrent delivery of dexamethasone and VEGF for localized inflammation control and angiogenesis. *J Control Release.* 2007;117(1):68–79.
- Wang J. Carbon-nanotube based electrochemical biosensors: a review. *Electroanalysis.* 2005;17(1):7–14.
- Wang J, Zhang X. Needle-type dual microsensor for the simultaneous monitoring of glucose and insulin. *Anal Chem.* 2001;73(4):844–7.
- Scheller FW, Schubert F, Neumann B, Pfeiffer D, Hintsche R, Dransfeld I, Wollenberger U, Renneberg R, Warsinke A, Johansson G, Skoog M, Yang X, Bogdanovskaya V, Buckmann A, Zaitsev Yu S. Second generation biosensors. *Biosens Bioelectron.* 1991;6(3):245–53.
- Binyamin G, Chen T, Heller A. Sources of instability of 'wired' enzyme anodes in serum: Urate and transition metal ions. *J Electroanal Chem.* 2001;500(1-2):604–11.
- Cass AE, Davis G, Francis GD, Hill HA, Aston WJ, Higgins IJ, Plotkin EV, Scott LD, Turner AP. Ferrocene-mediated enzyme electrode for amperometric determination of glucose. *Anal Chem.* 1984;56(4):667–71.
- Foulds NC, Lowe CR. Immobilization of glucose oxidase in ferrocene-modified pyrrole polymers. *Anal Chem.* 1988;60(22):2473–8.
- Gregg BA, Heller A. Cross-linked redox gels containing glucose oxidase for amperometric biosensor applications. *Anal Chem.* 1990;62(3):258–63.
- Gregg BA, Heller A. Redox polymer films containing enzymes: 2. glucose oxidase containing enzyme electrodes. *J Phys Chem.* 1991;95(15):5976–80.
- Hoet PH, Bröske-Hohlfeld I, Salata OV. Nanoparticles - known and unknown health risks. *J Nanobiotechnology.* 2004;2(1):12.
- Hurt RH, Monthieux M, Kane A. Toxicology of carbon nanomaterials: Status, trends, and perspectives on the special issue. *Carbon.* 2006;44(6):1028–33.

29. Morais JM, Papadimitrakopoulos F, Burgess DJ. Biomaterials/tissue interactions: Possible solutions to overcome foreign body response. *AAPS J.* 2010;12(2):188–96.
30. Bindra DS, Zhang Y, Wilson GS, Sternberg R, Thévenot DR, Moatti D, Reach G. Design and *in vitro* studies of a needle-type glucose sensor for subcutaneous monitoring. *Anal Chem.* 1991;63(17):1692–6.
31. Geise RJ, Adams JM, Barone NJ, Yacynych AM. Electropolymerized films to prevent interferences and electrode fouling in biosensors. *Biosens Bioelectron.* 1991;6(2):151–60.
32. House JL, Anderson EM, Ward WK. Immobilization techniques to avoid enzyme loss from oxidase-based biosensors: a one-year study. *J Diabetes Sci Technol.* 2007;1(1):18–27.
33. Yang H, Chung TD, Kim YT, Choi CA, Jun CH, Kim HC. Glucose sensor using a microfabricated electrode and electropolymerized bilayer films. *Biosens Bioelectron.* 2002;17(3):251–9.
34. Galeska I, Kim TK, Patil SD, Bhardwaj U, Chattopadhyay D, Papadimitrakopoulos F, Burgess DJ. Controlled release of dexamethasone from PLGA microspheres embedded within polyacid-containing PVA hydrogels. *AAPS J.* 2005;7(1):E231–40.
35. Vaddiraju S, Burgess DJ, Jain FC, Papadimitrakopoulos F. The role of H<sub>2</sub>O<sub>2</sub> outer diffusion on the performance of implantable glucose sensors. *Biosens Bioelectron.* 2009;24(6):1557–62.
36. Nicholls P, Loewen P, Fita I. Enzymology and structure of catalases. In: Sykes AG, Mauk G, eds. *Heme-Fe proteins.* *Adv Inorg Chem.* 2001;51:52–106.
37. Watt BE, Proudfoot AT, Vale JA. Hydrogen peroxide poisoning. *Toxicol Rev.* 2004;23(1):51–7.
38. Vaddiraju S, Singh H, Burgess DJ, Jain FC, Papadimitrakopoulos F. Enhanced glucose sensors linearity using poly(vinyl alcohol) hydrogels. *J Diabetes Sci Technol.* 2009;3(4):863–74.
39. Heller A. Implanted electrochemical glucose sensors for the management of diabetes. *Annu Rev Biomed Eng.* 1999;1:153–75.
40. Yu B, Wang C, Ju YM, West L, Harmon J, Moussy Y, Moussy F. Use of hydrogel coating to improve the performance of implanted glucose sensors. *Biosens Bioelectron.* 2008;23(8):1278–84.
41. Cengiz E, Tamborlane WV. A tale of two compartments: interstitial versus blood glucose monitoring. *Diabetes Technol Ther.* 2009;11 Suppl 1:S11–6.
42. Gale EA, Bennett T, Green JH, MacDonald IA. Hypoglycaemia, hypothermia and shivering in man. *Clin Sci (Lond).* 1981;61(4):463–9.
43. Atkins P. *Physical chemistry.* New York: W.H. Freeman; 2009.